From stainless steel 'til atomic ordeal

Creating a research ready STM

Jesper Moes BSc.
3866009
Daily supervisor: T.S. Gardenier M.Sc.
Supervisor: dr. I. Swart
Second supervisor: Prof. dr. D.A.M Vanmaekelbergh
Condensed Matter and Interfaces

2nd January 2019

Utrecht University

Abstract

Scanning Tunneling Microscopy (STM) is a technique with which the surfaces of metals, semiconductors and superconductors are investigated. A bias voltage is applied between the atomically sharp tip of the microscope and the surface of the sample. Through the tunneling of electrons between the tip and sample a constant current is established and the surface of the sample can be investigated. When using a new scanning tunneling microscope small vibrations can disrupt the delicate experiments. Sources of these vibrations can be external, such as pumps, or internal, such as vibrations leaking in from the computer. In this thesis we show how these vibrations can be investigated and reduced to $0.2pm$ peak to peak in order to make the microscope fully operational. Electrical wires, vibrations from the building and pumps have been found to be sources of these vibrations causing noise in the measurements. After reducing these vibrations it was shown that benchmark experiments could be conducted. These experiments include scanning tunneling spectroscopy, taking atomic resolution images and atomic manipulation. By comparing the results of the experiments to literature it can be confirmed that the results match and therefore results of upcoming research can be trusted.

Contents

1 Introduction

Scanning Tunneling Microscopy (STM) is a frequently used technique these days in research of metals, semiconductors, superconductors and more. [1] [2] [3] [4] The atomic resolution and possibility to be combined with Scanning Tunneling Spectroscopy (STS) give rise to the ability to examine the smallest details of the sample. The 1986 Nobel prize in physics was awarded to Dr. Gerd Binnig and Dr. Heinrich Rohrer for the design of the first scanning tunneling microscope. [5] Since then the technique has come a long way and STM's are commercially available from companies such as Scienta Omicron and HRK. Sigma Surface Science is a new company in the field. By creating new measuring heads, control systems and cryostats they are trying to design microscopes suiting the needs of the scientific community. In this report the bath cryostat STM of Sigma Surface Science shall be evaluated. It will be shown how one is able to use the full potential an STM. As is the truth for every new technology, one has to fix the little bugs and teething problems that are inevitably present in new apparatus. With the ability to do research at the atomic scale these little issues can already be a large problem in terms of results as will be shown later in the report. Fixing problems is key to reach the full potential of a machine but in order to perform all the experiments the researcher wants it is also important to equip the system with attachments specifically designed for certain investigations. All of these specific attachments and solutions to problems shall be discussed in this report on the Ultra-High Vaccuum (UHV) bath cryostat SPM of Sigma Surface Science they have named the POLAR. Cu(111) and Pb(100) crystals have been used . First these crystals have to be prepared and the noise has to be reduced.

A Cu(111) crystal will be used to do most of the benchmark experiments on as copper crystals have been extensively investigated over the years. It is known how to prepare the surface and it is known that copper has some interesting features in it's band structure. The first one of these features in the band structure of Cu(111) is a surface state at $-450mV$. All noble metals' (111) surface [6] [7] have a surface state similar to this. This electronic state is an occupied state in the electronic band structure of the surface Brillouin zone at point Γ. Electrons occupying this state can only scatter into the bulk if they change their momentum and/or energy. As shown already in 1994 by Hormandinger, the surface state of Cu(111) can be visualized by STS [8]. This is a good benchmark to investigate whether the STS on the POLAR microscope works properly. The second reason for using Cu(111) is that artificial lattices can be built on a copper surface using CO molecules. This has been done by Gomes *et al.* and Slot *et al.* [9] [10] These artificial lattices have not yet been investigated in a magnetic field, which can be a very interesting field of research due to potential Zeeman splitting of energy levels.

Pb(100) is not as well investigated as Cu(111) but it has interesting properties, like superconductivity and strong spin-orbit coupling. Since it hasn't been investigated as thoroughly as Cu(111) it is possible that it will be difficult to work it but the possible interesting researches that could be conducted on lead outweigh the possible problems. First of all lead is a superconductor at sufficient low temperatures [11]. Below $7.2K$ lead will turn into a type 1 superconductor. A type one superconductor can only conduct currents with zero resistance if the external magnetic field is below a critical level. Furthermore there has to be no internal magnetic field. These restrictions make that type 1 superconductors have been of limited usefulness thus far. Nonetheless they are of interest in the scientific world and maybe at some point a more practical use will be found. The second interesting feature of lead is that is has strong spin orbit coupling. Lead is much heavier than copper meaning the spin orbit coupling is much stronger. This spin orbit coupling makes for less scattering to the bulk, making for less broadening in STS spectra. [12]

2 Introduction of the POLAR UHV STM

Let's first have a look at the microscope, shown in figure 1, and focus on the features that make this STM different from other microscopes currently on the market. There are two types of cryostats with the capability of lowering the temperature of the measuring head to $4.5K$, flow cryostats and bath cryostats. Flow cryostats rely on a flow of liquid helium through the system in which the measuring head is placed. With a stable flow of liquid helium, a stable temperature can be achieved. However this flow usually causes noise in the system and the temperature can fluctuate. The POLAR STM therefore uses a bath cryostat to lower the temperature of the measuring head to $4.5K$ (liquid helium temperature). This cryostat is shown in the left of figure 1 and looks like a large stainless steel barrel. To reach the low temperatures, the measuring head is surrounded by the cryostat which is filled with liquid helium. To make sure the helium does not evaporate within hours, the vessel containing the helium is surrounded by another vessel containing liquid nitrogen. Van der Lit *et al.* [13] designed a cryostat in which the liquid helium can last for 2.5 days until the helium has evaporated and the machine (including the measuring head) starts to warm up. When no experiments are running the microscope will stay cold for 2.5 days which means the system will stay cold over the weekend, which is nice for the researchers. The new POLAR STM has no such problem as the manufacturers have managed to create a cryostat in which the helium will only evaporate at a rate of about 1 litre per 24 hours. Considering the vessel containing the liquid helium has a capacity of 10 litres this logically means that it only has to be filled every 10 days. This allows for better planning for the researchers, as well as less problems when important measurements are running. When an experiment is running longer than liquid helium is present in the bath cryostat, the tip is retracted a little bit and the cryostat can be filled without the tip crashing into the sample. There is one drawback of the POLAR STM, and that is the holding time of the liquid nitrogen. The liquid nitrogen is needed to keep the liquid helium as cold as possible to make sure it indeed holds for 10 days. In this machine the liquid nitrogen evaporates in 3 days. This means that it is still necessary to fill the nitrogen every 3 days and therefore handle the machine. It is however still a big advantage to have a long holding time for helium as filling liquid helium requires more time. Another disadvantage of filling helium in comparison to filling nitrogen is that the transfer line used for filling helium is inserted into the microscope and can therefore introduce more vibrations to the measuring head and crash the tip.

The second interesting feature of this machine is the vertical magnetic field which can be applied to the measuring head of the microscope. A $5T$ magnetic field can be activated and this can lead to new possibilities in terms of research. This is all placed in a stainless steel body which allows for ultra high vacuum, down to $10^{-11}mbar$. In order to reach these low pressures a couple of pumps are used: an ion pump, Titanium sublimation pump (TSP) and turbo pump for every chamber. The turbo pumps are used when relatively high pressures have to be reached, for example during evaporation of material or leaking in argon for crystal preparation. These turbo pumps are switched off after the pressure has dropped again, to $10^{-10}mbar$ as the vibration produced by these pumps can interfere with the measurements in the microscope. Furthermore this machine is highly adaptable in terms of personal requests of the researchers using the machine. There are many ports attached to all sides of the entire microscope which can be used to attach all kinds of measuring equipment. On this STM a 4-pocket evaporator (shown in figure 1 in the middle of the image pointing downwards) and ion gun are attached to the preparation chamber and a leak valve connected to a bottle of CO at the STM chamber.

An important part of such a machine is the software which controls the microscope. The software delivered with the POLAR STM is called SXM software and is also a new program with some bugs. The bugs encountered during the the year of research have been fixed by the

software developers of Sigma Surface Science and shall therefore not be treated in this report.

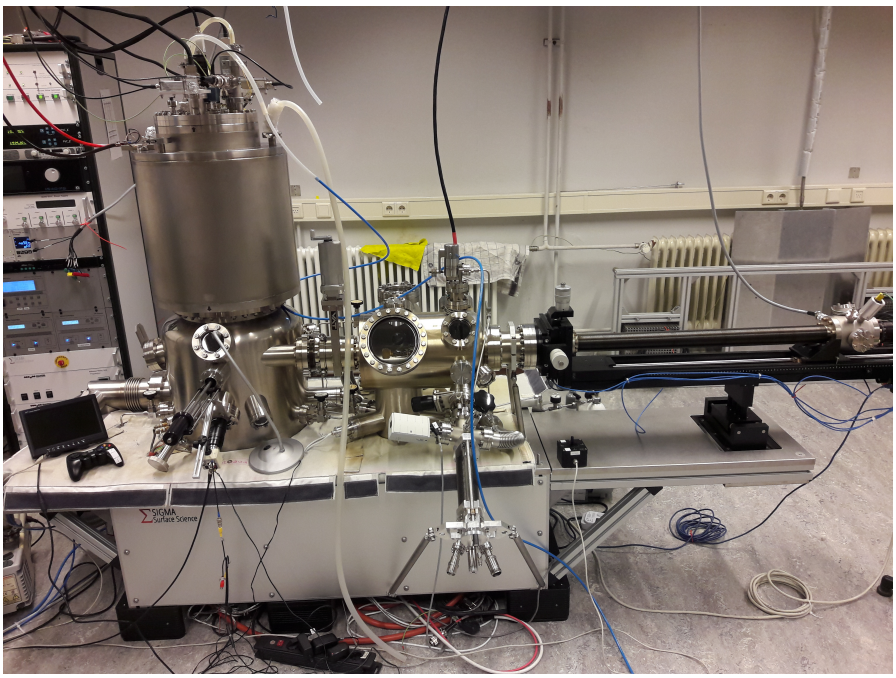

Figure 1: Photograph of the POLAR UHV STM as it is currently standing at the condensed matter and interfaces group in Utrecht

3 Theory

In this report it is assumed that basic knowledge of the workings of an STM are known to the reader. A detailed description can be found in many books and courses and shall therefore not be repeated in this report. [14] [15] Nonetheless a short summary of some important theory used in this report for the benchmark experiments shall be discussed below.

3.1 Scanning tunneling microscopy

Scanning Tunneling Microscopy is a useful technique in the analysis of semiconductors and metals. [1] [2] [14] An atomically sharp tip is approached to the surface of the sample. By applying a bias voltage tunneling current between tip and sample is created when the tip is close enough. The microscope can be setup in two different ways, constant current and constant height mode. In order to maintain a constant current a feedback loop is used. This feedback loop monitors the current and adjusts the height of the tip accordingly to keep the current stable. When the feedback loop is opened the tip will maintain a constant height, this is used when doing spectroscopy and shall be explained in the next section. Constant current mode is used while scanning as the feedback loop will ensure the tip retracts when scanning over high objects on the crystal surface. While scanning over the surface, every change in height on the surface changes the tunneling current, the tip reacts by adjusting for this such that the tunneling current remains stable. This reaction leads to a change in height of the tip and this is interpreted by software and can than be shown as a height profile or topology image. Since the end of the tip is, ideally, only one atom in size this can lead to resolution up to the point where individual atoms and molecules can be distinguished.

3.2 Scanning tunneling spectroscopy

An important tool in the world of Scanning Tunneling Microscopy is Scanning Tunneling Spectroscopy (STS) [16]. STS allows the researcher to examine the electronic structure of a specific location on the sample. After positioning the tip, the bias voltage is set at a constant voltage and the feedback loop is opened. As mentioned before the tip shall maintain a constant height if the feedback loop is opened. When scanning the feedback loop is always closed because large height differences in the sample would crash the tip in the sample. After this a range in voltage is set over which the researcher wishes to investigate the sample. The current is measured and from this a I/V spectrum is created. The derivative of this spectrum is used more in research as the dI/dV is directly related to the local density of states (LDOS) of both the sample as well as the tip. The fact that one measures both the tip and the sample can be both an interesting feature to investigate as well as a problem in the desired measurements [17] [18]. A lock-in amplifier is used to directly record the dI/dV signal instead of numerically calculating it from the I/V spectrum. The lock-in amplifier applies a small sinusoidal modulation in the bias voltage which in turn creates a small sinusoidal response in the tunneling current. The amplitude of this response is directly influenced by the slope of the I/V signal. The signal is passed through a low pass filter which filters out signals with a frequency higher than a predetermined limit. This process significantly increases the signal to noise ratio with comparison to the mathematically derived dI/dV spectrum. [16] [19] An interesting example of a dI/dV curve is a curve of a noble metals (111) surface [6] [7]. Noble metals have a so called surface state. This electronic state is an occupied state in the electronic band structure of the surface Brillouin zone. Figure 2 shows a dI/dV spectrum of Ag(111) and the corresponding band structure. how the peak of the spectrum originates from the electronic surface state in the band structure. Electrons occupying this state can only scatter into the bulk if they change their momentum and/or energy. [7]

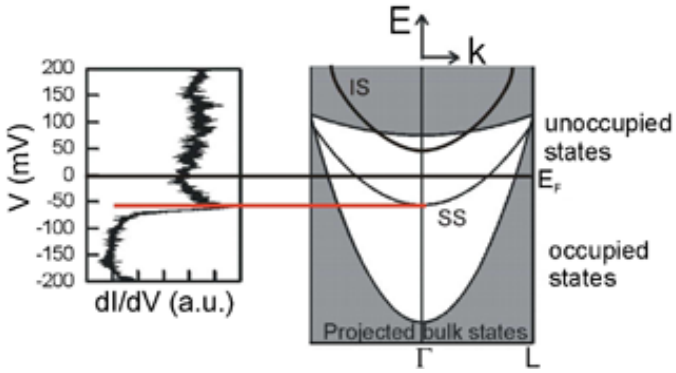

Figure 2: The surface state of Ag(111). Left: dI/dV spectrum taken by STS on Ag(111) showing a peak at -69mV. Right: Schematic representation of the surface state in the band structure. [7]

As mentioned, the dI/dV curves are proportional to the LDOS and are therefore an important tool in understanding the artificial lattices. In equation 1 this proportionality between dI/dV signal and the LDOS is shown.

$$\frac{dI}{dV} \propto \rho_s(E_f - eV) \cdot \rho_t(E_f) \tag{1}$$

In this equation ρ is the density of states (DOS) of either the tip (t) or the sample (s), E_F is the Fermi energy and eV is the bias voltage. A high signal in the dI/dV spectrum indicates a larger amount of electrons tunneling at that energy, which means a higher LDOS as it is measured at one point of the sample. This includes the DOS of the tip and the DOS of the sample. A spectrum taken on the substrate will therefore always be influenced by the DOS of the tip. When a different material is deposited on the substrate it is possible to remove both the DOS of the tip as well as the DOS of the substrate and only measure the DOS of the adsorbate. By dividing the spectrum taken on the adsorbate by the spectrum taken on the crystal surface, the spectrum that remains is only the DOS of adsorbate [17]. An important requirement for this to work is that the tip isn't changed in any way when both spectra are recorded. This technique is very useful when one is looking at specific points in artificial lattices and therefore the benchmark experiments on STS shall be important to see if the STM works as desired and the spectra taken can be trusted in further research.

3.3 Atomic manipulation using scanning tunneling microscopy

In 1990, Eigler showed that it was possible to manipulate individual atoms the surface of a substrate using an STM. [20] He did this by recreating the name of the company he was employed by, IBM. 3 years later Eigler teamed up with Crommie from the university of Berkeley and showed that the manipulation of atoms using STM was not just a fun trick but was actually useful for the scientific world. They built a quantum coral by placing Fe atoms in a ring on Cu(111) and in the process showed that surface state electrons of the Cu(111) could be confined. [21] This has been used and refined ever since and is for example used by Gomes *et al.* as well as Slot *et al.* [9] [10] to create artificial lattices and is called lateral manipulation, but this is not the only method of manipulating atoms using an STM tip. It is also possible to do vertical manipulation, using this method one approaches the tip of the STM to the atom or molecule

one wants to manipulate and lifts this particle of the surface. After one moves the tip and particle to the desired location one approaches the surface with the tip and drops the particle back on the surface [22] [23]. In this research this method is not used because of two issues. First of all, it is very difficult to reproducibly pick up one particle and place it back on the surface with high accuracy. Secondly it is hard to detach the particle from the tip after the manipulation is completed. Lateral manipulation employs a somewhat similar technique, the tip of the STM is approached to the adatom but instead of lifting the particle, the tip approaches the adparticle and while maintaining the close distance moves over the surface dragging or pushing the particle along as shown in figure 3. To approach the tip to the surface the bias voltage is decreased and the tunneling current is increased. Meyer *et al.* [24] already reported in 1997, using the lateral manipulation method, settings for manipulating CO molecules and Pb atoms on a Cu(211) surface at temperatures of 15 to $80K$. For the manipulation of Pb atoms they used a resistance of 400 - 600 $k\Omega$. To put this in context this is compared with the values of the paper of Slot *et al.* [10]. in which they manipulate CO on a Cu(111) crystal. The parameters used in that paper are $10mV$ for the bias voltage and $40nA$ for the setpoint current. Using $R = \frac{U}{I}$ with R the resistance, U the bias voltage and I the tunnel current, the resistance is calculated to be 250 $k\Omega$. In this research the temperature is $4.5K$, thus taking this difference in temperature into account it was decided to initially use the 250 $k\Omega$ settings for manipulating CO molecules on Cu(111) and on Pb(100). If manipulation turns out to be unsuccessful the current, and therefore the resistance, shall be increased.

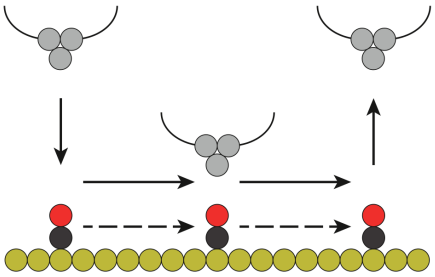

Figure 3: Schematic representation of lateral manipulation using a Scanning Tunneling Microscope. Cu atoms of the substrate are shown in yellow, the black atoms represent carbon atoms and oxygen atoms are shown in red [25].

4 Results and discussion

In order to investigate whether the machine is working in such a way that the results can be trusted, it is necessary to do a set of benchmark experiments. These experiments will be described in this section and involve noise reduction, taking images with atomic resolution and taking spectra on copper and lead. These benchmark experiments will be compared with known literature and with the previous knowledge of the group, to investigate whether the results match and further results can be trusted. The exact methods and settings in order to achieve these results in the benchmark experiments and therefore the methods on how to use the machine for new research have been documented in a manual. This manual was written largely by the author and a digital copy is available upon request. The software used for the manual is OneNote as this is a convenient program which can be used whilst operating the Sigma Surface Science POLAR STM. This program does not convert well to LaTeXand is therefore not included as copy in the supplementary information.

4.1 Crystal preparation

When starting experiments in an STM, whether used or new, is to clean the crystal one is going to investigate. In this case a Cu(111) and Pb(100) were used to investigate the capabilities of the POLAR. Cu(111) has been investigated by many groups and therefore the procedure for this is well known. The crystals were ordered from Surface Preparation Laboratory (SPL) and then placed into the vacuum. It does not require any additional cleaning steps before inserting the sample into the vacuum. The Cu(111) crystal is cleaned by annealing and sputtering steps. The annealing step is to ensure that the surface smooths out by heating up the crystal and the sputtering steps are to clean particles off the surface by means of shooting ions at the crystal. The exact settings are different per microscope, for this machine and crystal we have decided to anneal it to $600C^o$ for 5 minutes. This is alternated with 15 minute sputter sessions using $8.5 * 10^{-6}mbar$ ($2 * 10^{-10}mbar$ base pressure) of argon which is ionized and accelerated towards the Cu(111) crystal with $3kV$ and $10mA$. These two steps are alternated for at least 3 cycles to clean the crystal. The last sputter step is done at $1kV$ instead of $3kV$, this gives less energy to the ions. The last anneal step is only heated to $550C^o$. By keeping the temperature lower, defects from deeper within the crystal do not surface thus leaving a cleaner surface with less defects. Cleaning a Pb(100) crystal is less trivial, which is one of the reasons why Pb(100) is not used as much for research. The biggest problem with lead is that it is a much softer crystal than for example copper. A cleaning procedure using acetic acid and aceton, before putting it in the vacuum of the STM, was experimented with before with little success. [26] A cleaning procedure using only sputtering with Ar ions and annealing was decided upon. The settings to do this were changed, with respect to the cleaning procedure of Cu(111), as the Ar ions could damage the crystal structure of the Pb(100) due to the softness of the crystal. The melting point of lead is also lower than the melting point of copper thus the annealing temperature was adjusted. We chose to anneal to $200C^o$ and sputter with $0.75kV$ and $10mA$ for 30 minutes. Since lead is also much more reactive than copper the decision was made to clean the crystal for multiple days. This resulted in more than 20 cycles of sputtering and annealing. As will be later shown, this was proven to be effective. If the crystals come from ambient conditions and are prepared for the first time the procedure has to be repeated multiple times as there is more dirt on the crystal. Once they have been cleaned it is easier to remove the dirt and irregularities. It was decided that the Cu crystal would only need one or two cycles to be cleaned and the Pb crystal would need about five cycles.

4.2 Noise reduction

A clean crystal is a good start however this does not mean that one can immediately make nice STM pictures. Two factors are very important to make good STM pictures, the first is a sharp tip and the second factor is low noise levels. The first factor is a problem that has haunted the STM community for years, there does not seem to be a good procedure to get a reliable tip. For now the way to sharpen a tip is to either apply a quick bias pulse through the tip or poke the tip a couple of nanometres into the surface. Some have tried to quantify how a certain tip sharpening procedure changes the tip but this is still debatable. [27] In contrast, reducing noise levels is not difficult but it is very important. Every little vibration coming from pumps, electronics and all other sources can be isolated and one can think of a solution to remove these noises.

First step in noise reduction is to distinguish which kind of frequencies are interrupting with the signal of the STM. We scan in single point mode, which means the tip is not scanning across the sample but instead is hovering stationary at one point maintaining the reference feedback current. This way all the vibrations the tip "feels" come from outside noise. The integrated oscilloscope is now used to identify the different frequencies and one can identify where they come from by changing one thing on the machine and doing the same single point measurement again. The changes that can be made are for example, turning off attached electronics like the helium depth indicator, or grounding certain contacts. The vibrations measured are not directly relatable when looking at the oscilloscope, however the built-in oscilloscope has the option to perform a Fourier transform of the signal and with that transform the signal into a frequency measured in hertz.

Figure 4a and 4b show a cropped version of the built-in oscilloscope and the Fourier transformed signal. In black the signal of the height trace is shown and in red the signal of the current. We have focused on the red signal for the noise reduction measurement but it should be very similar when looking at the black height noise signal. In figure 4a a peak is shown and the cursor (black vertical line) is placed on top of the peak to determine the frequency and amplitude of this noise. In the bottom right corner the frequency in hertz is shown to be $389.4Hz$, in the bottom left the amplitude for the height trace is shown, which is $16nm$ and right of that is the amplitude of the current noise and this is $6.325nA$. Normal settings to scan are a reference current of 1nA and therefore a noise of $6.325nA$ will significantly alter the signal and measurements taken with this noise are not reliable. The source of this noise was the lock-in amplifier for doing STS, the lock-in amplifier applies voltage amplitude with a certain frequency to the tip for the measurements. The oscilloscope can be turned off in the software, eliminating this noise from the measurement. In figure 4b the source of the noise was removed and the signal seems much noisier, this is because of scaling. Scaling changes the size of the y-axis in the built-in oscilloscope in order to visualize the smaller noise signals. This signal changes with every measurement as the noise that is left does not have a specific frequency but rather a broad range of frequencies. These are mostly due to natural vibrations of the tip and machine and these can not be eliminated. The numbers in the bottom left show the amplitude of the noise at the marker, $1.170pm$ and $636.3fA$ for the topo and current respectively. This is a much lower level and shall therefore interfere significantly less with the measurements. In table 1 the noise created by the lock-in amplifier, has not been implemented as the frequency changes depending on the value you enter in the SXM software. Table 1 shows the different frequencies found using this procedure with the POLAR UHV STM and the solutions to reduce or eliminate the noise.

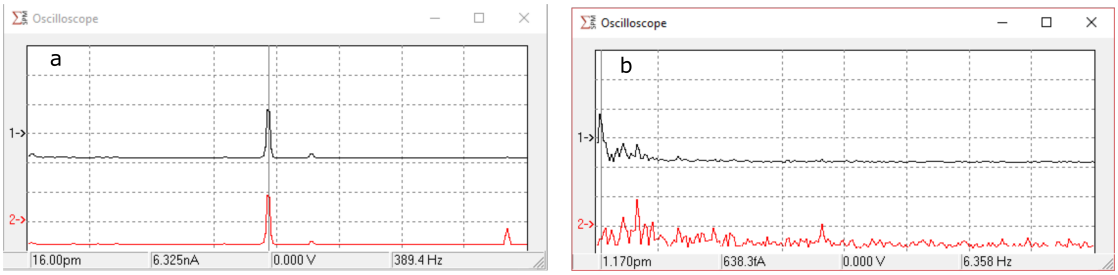

Figure 4: Cropped image of the Fourier transform of the signal shown in the built-in oscilloscope of the SXM software, (a) A peak is visible at $389.4Hz$, created by the lock-in amplifier. (b) The source of the noise has been eliminated reducing the noise level.

Table 1: Noise identification, using the Fourier transform of the signal, and solutions for noise reduction

Frequency (Hz)	**Determined source**	**Solution**
1-10	Natural movement of the building	Active vibration dampening feet installed
50	Helium depth indicator	Turned off He depth indicator
50 & 300	Oil pump for CO line	Turned off pump
68 & 136	Stage not released properly	Raised the measuring head
80	Turbo pump	Turned off turbo pump
100	Temperature controller	Pi filter attached at temperature controller feed-through
50kHz	Leaking in from the computer via the bias voltage feed-through	50kHz filter attached
Other high frequency noise	Leaking in from the computer and stepper motor through electronic feed-throughs	Changed to cable with ferrite cores and turned off stepper motor

The first and most prominent frequency, or rather range of frequencies, are the 1 to $10Hz$ frequencies corresponding to the natural movement of the building. When such a sensitive machine is placed in a quite old building movement of the building will always be a problem as it was not built for low noise experimentation. Ideally an STM is placed in a building with a floor disconnected from the rest of the building. Before the installation of the POLAR STM it was already known that a separate floor would not be possible and to limit the noise from the building a different solution was found. Active vibration dampening feet were installed beneath the machine to reduce the vibrations caused by the building. Active vibration dampening works just like noise canceling headphones, they measure the frequency of the noise and produce a counter signal to dampen the noise. In this case three of these feet were installed to dampen the noise as much as possible. In figure 1 these feet are visible beneath the entire system as three black boxes. The second source of noise was discovered to be the helium depth indicator with a frequency of $50Hz$. By simply turning off the indicator the noise disappeared, since the rate of evaporation was monitored over the course of a couple of months it was shown that this matches the 1 litre per day evaporation rate predicted by Sigma Surface Science. Using this knowledge

the helium depth indicator can be turned off during use and only be turned on shortly in the morning to check if there isn't any abnormal change in the evaporation rate.

Multiple different frequencies originated from two turbo pumps used to create and maintain the UHV in the microscope. One additional oil pump is used to flush the carbon monoxide line if needed. All of these pumps are usually not in use when doing experiments. The 68 and $136Hz$ noise problems were quite prominent throughout a couple of measurements on multiple different days. The measuring head was not lifted properly into the cryostat and was therefore in contact with the bottom of the cryostat. When the measuring head is lifted properly it hangs in springs which dampen vibrations in the microscope. Not lifting the measuring head was a fault of the researchers, however it is important to know what kind of frequency is present in the system when such a mistake is made. For future reference if these frequencies are measured again whereas the stage was lifted properly this could mean a problem with the lifting mechanism.

The temperature controller used on the POLAR STM also caused vibrations in the measurements. $100Hz$ noise leaked in via the electronics cable connecting the STM to the temperature controller. A filter was installed between the cable and the feed-through at the microscope to filter out low frequency noise coming from the controller. Disconnecting the temperature controller would also suffice however this would mean connecting and disconnecting the cable on a daily basis and this might cause wear to the connection.

High frequency noise is difficult to investigate as it isn't shown in the built-in oscilloscope and is therefore taken care of by the developer before installing the microscope. Unfortunately it is always possible for the developer to miss one or two of these frequencies. This is not a problem for the normal scanning mode, however it is possible that this kind of noise has a negative effect on spectra taken with STS. These problems presented itself while trying to measure the superconducting gap of the Pb(100) crystal, which shall be discussed later in the report. An employee from Sigma Surface Science helped to investigate the sources of the high frequency noise and together, solutions to the problem were found. The first source turned out to be the stepper motor which is used to move the manipulator arm, this is easily fixed by turning off the stepper motor when taking spectra. The second source was found to be coming from the computer and leaking in via the cable of the bias voltage. Two solutions were found to effectively dampen this noise. The cable was exchanged for a cable with ferrite cores attached to it, and an additional high frequency filter was attached at the feed-through.

After the reduction of the noise it was possible to take a single point measurement with a noise level of $0.2pm$ peak to peak shown in figure5. A dY is shown of $78.90fm$ per segment, the blue measurement has the largest peak to peak distance and is therefore the noisiest. We can now calculate the peak to peak noise level: $2.5 * 78.90 \approx 200fm$ or $0.2pm$ was reached after noise reduction. This is a level which will not significantly interfere with any measurements. To give an indication, the imaged size of a Cu molecule in the Cu(111) lattice, in the STM, is $255pm$. Therefore the noise level is 0.1% of a Cu atom.

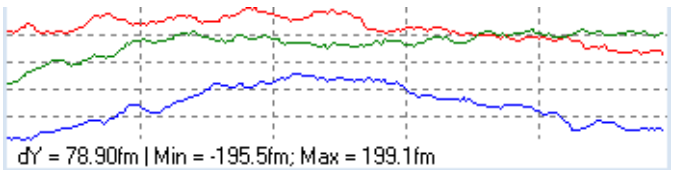

Figure 5: Single point measurement after reducing all the noise. Every line represents a single point measurement and therefore the peak to peak distance of the blue line is $0.2pm$

4.3 Atomic resolution

After the crystals are clean and flat, and the noise level is as low as possible, atomic resolution images of the crystal can be taken. The reason to investigate atomic resolution images of a crystal is to determine the angle of the crystal. Every crystal is placed differently onto the sample plate and therefore the exact angles for the closed packed rows of the crystal are different per sample. It is useful to know this angle in order to correct for this while building a lattice. This correction can be done in the software in order to determine the exact locations where the adparticles should go. This is especially useful since it is usually not possible to have atomic resolution while also scanning particles on the surface due to a limit in resolution. Figure 6a shows the atomic resolution of a Cu(111) crystal including the crystal structure inserted. From this image the angle of the closed packed row of the Cu(111) was determined to be 23.5 degrees. Figure 6b shows the Pb(100) crystal, in which the close packed row is nearly level with the horizontal line of the scan window. An interesting addition of the image of the Pb(100) crystal is the step edge on the right hand side of figure 6b. The atoms on the far right of the image are one layer lower than the atoms on the left, in an STM image this is visible as a darker colour tone. Lastly in figure 6c and d a monolayer of CO molecules is shown. This monolayer was deposited on a Cu(111) crystal and was part of an experiment to deposit carbon monoxide molecules on the crystal surface as will be explained in more detail in the next section.

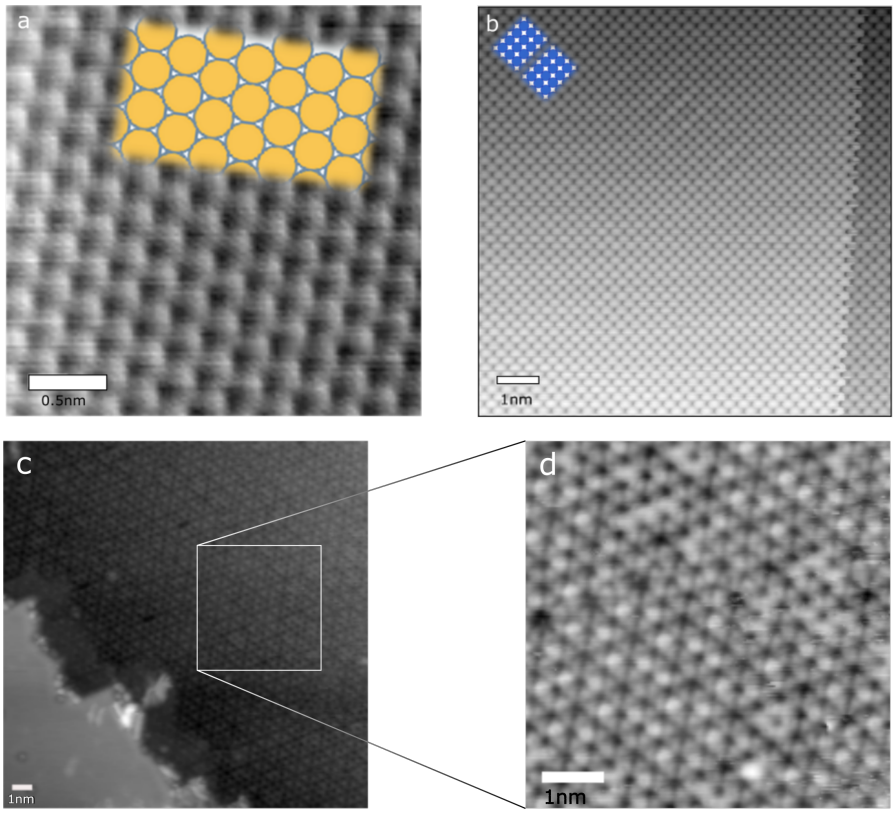

Figure 6: Atomic resolution images of (a) Cu(111) and (b) Pb(100) with inserts of a schematic atomic lattice. (c) CO monolayer on top of a Cu(111) surface. (d) Zoom in of the CO monolayer revealing the hexagonal phase.

4.4 Atomic Manipulation

The noise levels have been reduced and the crystals are clean, the next step to take to ensure that the machine is fully functional for our upcoming research is atomic/molecular manipulations. The first thing to do is evaporate carbon monoxide onto the crystal, with which the lattices will be build. For still unknown reasons CO shows up as a depression on the Cu(111) surface. On, for example, Au(111) it shows up as a protrusion. [28] The multiple shields around the cryostat, that make sure the holding time for the helium is ten days, are aligned such that there is a line of sight to the crystal from the leak valve. As the chamber is at room temperature and the crystal is at roughly $4.5K$, the crystal (and measuring head) will act as a cryo-pump ensuring that the CO will indeed end up at the crystal. In a new microscope the exact settings of how much CO should be evaporated in the SPM chamber to get a certain coverage is unknown, therefore this is a trial and error situation. One of the first attempts, using a pressure of $3 * 10^{-6} mbar$ ($6 * 10^{-10} mbar$ base pressure) for 60 seconds, showed a coverage shown in the previous section in figure 6c. This was determined by Wortmann *et al.* [29] as a CO monolayer on copper, visible by the hexagonal structure As it is impossible to manipulate individual CO molecules this way, therefore the procedure to evaporate CO should be adjusted to get a lower coverage on the Cu(111) crystal. The pressure was adjusted to $1 * 10^{-8} mbar$ for 90 seconds and a lower coverage of CO molecules was achieved, as shown in figure 7a. Individual molecules are visible and the monolayer has been removed. Depending on the lattice one wants to build one can opt to deposit more CO. A higher coverage is preferable as one does not have to move hundreds of nanometres to collect the amount of molecules necessary. The difficulty with determining the dosage of CO on the crystal as a function the pressure is that the exact pressure when leaking in CO is not the only variable. The difference between the base pressure and the pressure when leaking in CO is more important. When the base pressure is already in the $10^{-9} mbar$ range the coverage will be less than when the base pressure is in the $10^{-10} mbar$ range.

The software window shown in figure 7b is the lateral manipulations window of the SXM software used for this STM. The development of this part of the software was finished September 2018. In this window settings can be changed which make it possible to execute lateral manipulations. The first important setting is the speed at which the tip moves. The usual speed of the tip while scanning is about 10-20 nanometres per second. While doing manipulations it is imperative that the tip moves slower, a speed in the order of $1nm/s$ has turned out to work for this microscope. Moving the tip too fast can result in the detachment of the adatom halfway through the manipulation, or the tip just moves over the molecule and does not drag it along at all. Without the option in the manipulation tool to change the speed, one would have to manually change the speed of the tip after every manipulation which takes too much time for efficient building of lattices. The next setting in this window of interest is the possibility to add a confirmation trace after the manipulation. This can be used to confirm if the manipulation was successful or not. To do this the tip goes back to it's original scanning settings and retraces the manipulation line and shows the height difference of the trace. As the CO molecule shows up as a depression the height trace shows a dip at the location of the CO and thus if the CO has moved, the dip should be visible at the end of the trace. The last important settings shown in figure 7b is the possibility to set the current and voltage setpoints and as mentioned before in section 3.3 changing these settings are necessary to approach the particle with the tip. For manipulations of CO on Cu(111) the same parameters are used as in the paper of Slot *et al.* [10]: $40nA$ and $20mV$. The settings for manipulating adparticles on Pb(100) will have to be discovered via trial and error as nobody has reported on this before. The settings that will be used in the beginning of the experiments will be the same as the ones for manipulating CO on Cu(111) and from there on adjustments can be made if necessary.

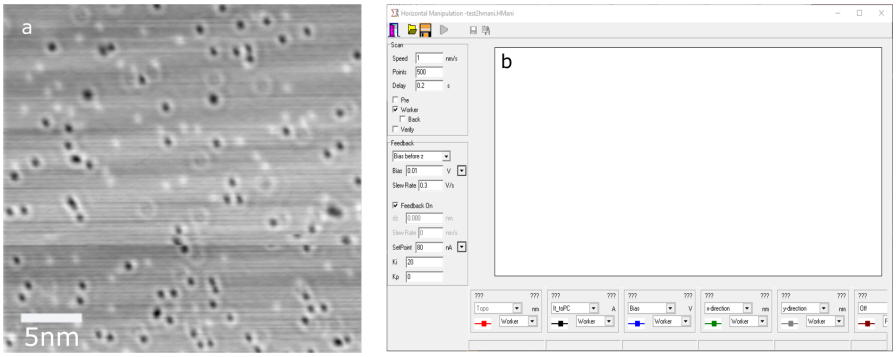

Figure 7: (a) CO molecules on a Cu(111) surface shown as black dots, with a decent coverage for building artificial lattices. (b) Lateral manipulation window of SXM software with options to change the speed of the tip, the setpoints, a delay and the possibility to visualize up to 6 channels.

Figure 8 shows a height trace of a successful manipulation. On the x-axis it shows the amount of points set in the software which can be converted to distance if desired. This is not necessary in building of lattices as we are generally only interested in the result and not in the manipulation itself per-se. The y-axis shows the height of the tip. This trace does supply valuable information, the 7 peaks shown in the trace mean that the tip has sudden "hops" pretty much at similar distances. These "hops" have been determined to be the CO molecule under the tip hopping from top site to top site of copper atoms in the crystal. Before the scan has crossed the location again with the confirmation scan it is possible to tell if the manipulation was successful, this is not the most reliable tool but it can help speed things up when building a lattice, as the confirmation trace takes time.

The first successful manipulations that created a diamond shaped structure that was built, in the POLAR STM, is shown in figure 9a. This is a lattice build using CO molecules on top of the Cu(111) crystal. An interesting observation is that all of the CO molecules which are normally imaged as a black dot now have a bright spot in the middle. This was shown to be a CO molecule on the tip by Bartels et al. [30] and it got attached on the tip during a manipulation attempt. This shows a drawback of atomic manipulation, getting a CO molecule stuck on your tip is a problem as it is virtually impossible to manipulate with a CO on the tip. Luckily this does not occur that often and it is easy to remove the CO molecule from the tip using a bias pulse. The creation of this lattice shows that atomic manipulations work and the settings reported in this section can be used in upcoming research. No further building was conducted as the tip changed after this image was taken but this is a proof of concept that the manipulation of CO molecules on a Cu(111) crystal works in this UHV SPM.

Investigations were conducted on Pb(100), because this material has not been the subject of much research. The reason is that lead is a very soft metal and it was hypothesized that manipulations on lead are impossible. CO was evaporated onto the crystal using the same settings as the evaporation on copper and particles were seen on the surface. Interestingly these particles are shown in the scan as protrusions instead of depressions, as on Cu(111). On Au(111) they are also shown as protrusions so this is not an anomaly. [28] Manipulations were attempted using the same current and voltage settings but the tip crashed often, thus the current was lowered from $40nA$ to $20nA$. Manipulations were working better for the lower current setting, the tip did not crash anymore. The drawback of a $20nA$ setting for the current is that only 10% of

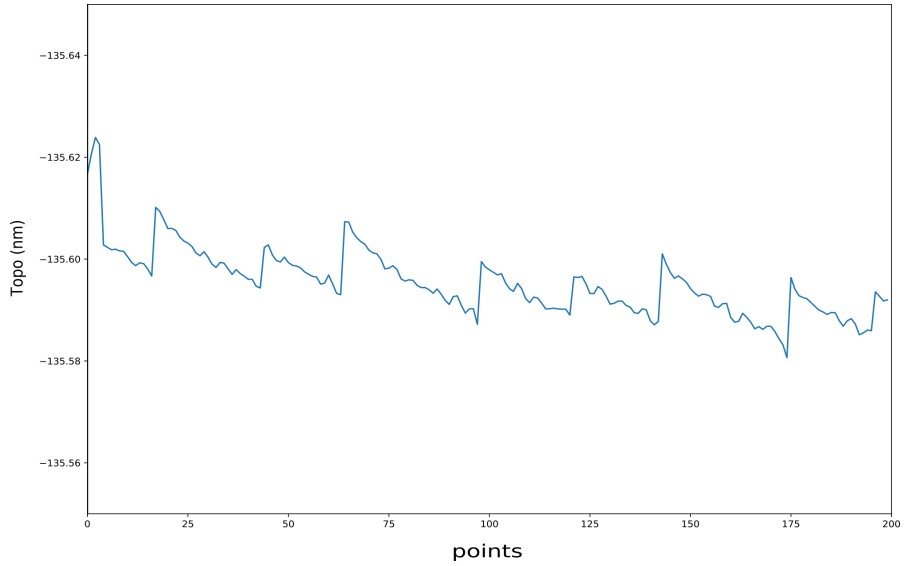

Figure 8: Height trace of the tip during a successful manipulation of a CO molecule on Cu(111) over roughly 2nm

the manipulation attempts was successful. In figure 9b and figure 9c a successful manipulation on Pb(100) is shown. The letter U was created after manipulating 7 separate particles were moved into place. In these pictures a couple of features can be seen which are of interest. Firstly at the bottom left of the U a black spot can be seen, this is a vacancy in the Pb crystal lattice. Where this atom has gone is uncertain but it could be that it is one of the particles in the U. This is an indication that the particles might not all be CO molecules. The second interesting feature is the shadow next to some of the particles, it is especially visible near the top two particles of the U. These shadows sometimes appear after a successful manipulation, it seems that the crystal lattice beneath the particles that are manipulated adjusts slightly. This coincides with the fact that sometimes atoms in the substrate, get pushed or pulled out of the crystal surface.

As there is controversy about the identity of the particles, it was decided to evaporate more CO onto the crystal to investigate the coverage. Even while evaporating at a pressure of $3 * 10^{-6} mbar$ ($6 * 10^{-10} mbar$ base pressure) for 1 minute, the same which led to a CO monolayer on Cu(111), a similar coverage of adparticles was found on Pb(100) after evaporating with the same pressures for 10 seconds. This is a strong indication that the particles on the surface of the Pb crystal are Pb adatoms and not CO molecules. To confirm this hypothesis a DFT simulation was run for CO molecules on Pb(100) and Pb(110). The results are shown in figure 10. In both simulations CO does not bind to Pb(100) or Pb(110) at all, which confirms the hypothesis that the adparticles are Pb adatoms and that manipulation of Pb adatoms is possible on a Pb(100) surface. Further research shall most likely not be conducted on Pb(100) as building a lattice will be difficult with the problems discussed previously.

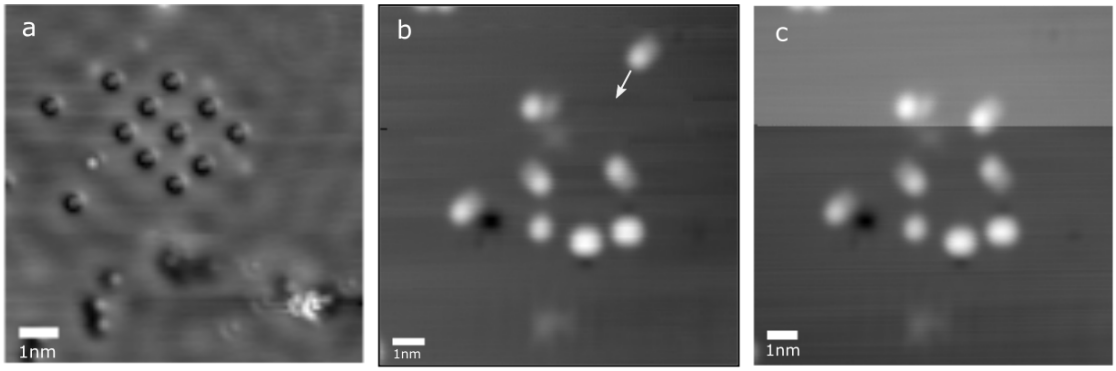

Figure 9: (a) Lattice built of CO molecules on a Cu(111) crystal, imaged using a CO tip. (b) Manipulation attempt of an adparticle on a Pb(100) crystal in the direction of the arrow. A vacancy in the crystal lattice is visible left of the U. Next to most adparticles shadows can be seen related to distortions in the crystal lattice. (c) Successful manipulation of an adparticle on Pb(100)

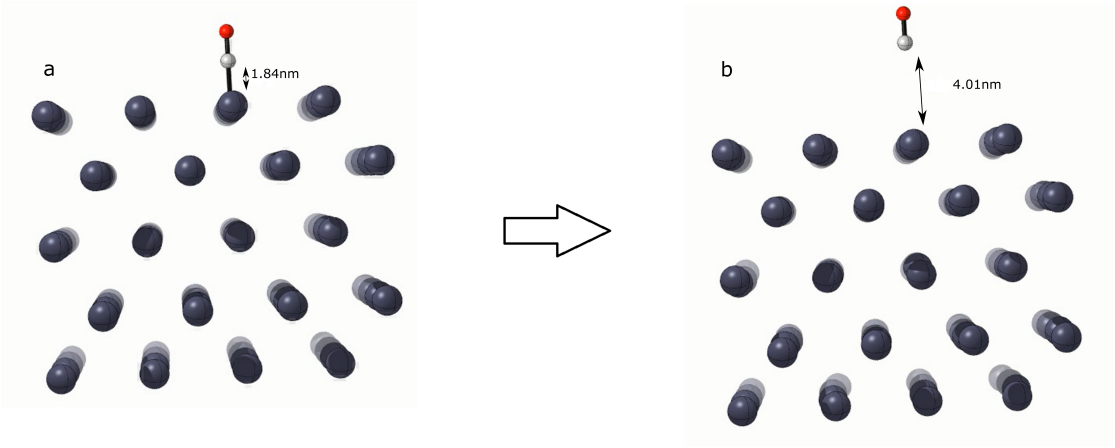

Figure 10: Screenshots of the simulation of CO on Pb(100) with Cu, C and O atoms showing in black, white and red respectively. Left: Initial starting settings with the C-Cu distance at $1.84nm$, these settings are the stabilized settings for a CO molecule on Cu(111). Right: After the simulation has ran the CO molecule moved away from the Cu crystal surface

4.5 Spectroscopy measurements

Hormandinger showed in 1994 that Cu(111) has a surface state around $-450mV$ and that this surface state can be visualized using STS. [8]. Figure 11a shows the dI/dV spectrum Hormandinger measured using STS. The research of Hormandinger was repeated on the POLAR STM and the result is shown in figure 11b. A sharp rise is visible in both spectra around $-450mV$ which corresponds to the surface state. There are some small differences when comparing the spectrum taken by Hormandinger and the spectrum taken on the POLAR STM. The reason for these small differences in the spectrum is that, as mentioned in section 3.2, STS is a technique that measures the LDOS of both the tip and sample, so every spectrum will be slightly different depending on the material and shape of the tip. A couple of conclusions were drawn from this benchmark experiment. Firstly it was confirmed that the remaining noise does not have a large effect on the spectrum. Secondly the settings used to measure this dI/dV spectrum are correct for spectra in this voltage range. Meaning that if a lattice has been built and spectra are taken around this energy range they can be used to get decent spectra. The settings which were investigated include the settings for the lock-in amplifier, delays and acquisition time. All of these settings for doing STS spectra in the range of -1 to $1V$ can be found in the manual.

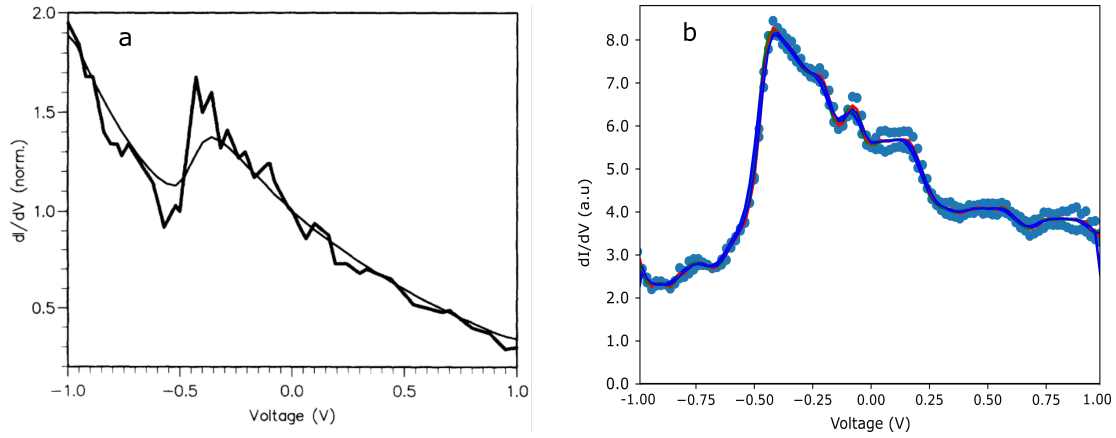

Figure 11: A surface state on Cu(111). (a) dI/dV taken with STS on Cu(111) showing a peak at $-450mV$, measured by Hormandinger *et al.* [8]. (b) dI/dV taken on Cu(111) on the POLAR STM showing a similar spectrum as (a). The red curve is a fitted curve to the data points and the blue curve is a smoothed fit.

We want to conduct experiments on lead and therefore it is important to do benchmark experiments on clean Pb as well. In 1994 Wurde *et al.* [31] theoretically showed the band structures of Pb (100) and Pb(110) and he showed that the surface states are very close to the bulk states and not in a range which is properly measurable with STS. There is, however, another feature in the band structure of lead which is of interest. This is a gap of a couple of mV around $0V$, called the superconducting gap. The origin of this gap is that two electrons form a Cooper pair and the energy gain from this formation is the gap near the Fermi energy. [32] The formation of a Cooper pair state of the electrons is the origin of superconductivity. This discovery and the theory behind it led to the Nobel prize in physics for John Bardeen, Leon Cooper and John Schrieffer. [32] [33]

Since the energy of this gap is so small, any noise might interrupt the possibility to visualize the superconducting gap in STS experiments. This is where the high frequency noise mentioned in

the noise reduction section 4.2 comes into play. While this noise was present the superconducting gap is not visible as shown in figure 12a. After the high frequency noises were quenched using a filter and a cable with ferrite cores, the gap could be observed, shown in figure 12b and 12b. The centre of the SC gap shown in figure 12b is not located at the $0V$ point, there could be multiple reasons for this. It is possible that the calibration was slightly off during the measurement, or that the tip had some instability while taking this measurement. At an earlier moment, while installing the filter and ferrite core cable, a dI/dV spectrum was recorded with the location of the SC gap indeed around the Fermi energy. This spectrum is shown in figure 12c. This spectrum was taken by Albrecht Feltz from Sigma Surface Science on the POLAR STM in Utrecht. The width of the SC gap in figure 12b and 12c were determined to be 6mV which corresponds to literature. [34] From these benchmark experiments it can be concluded that STS works as expected and the high frequency noise is reduced enough to do very sensitive measurements. The correct settings for different spectra were written down in the manual.

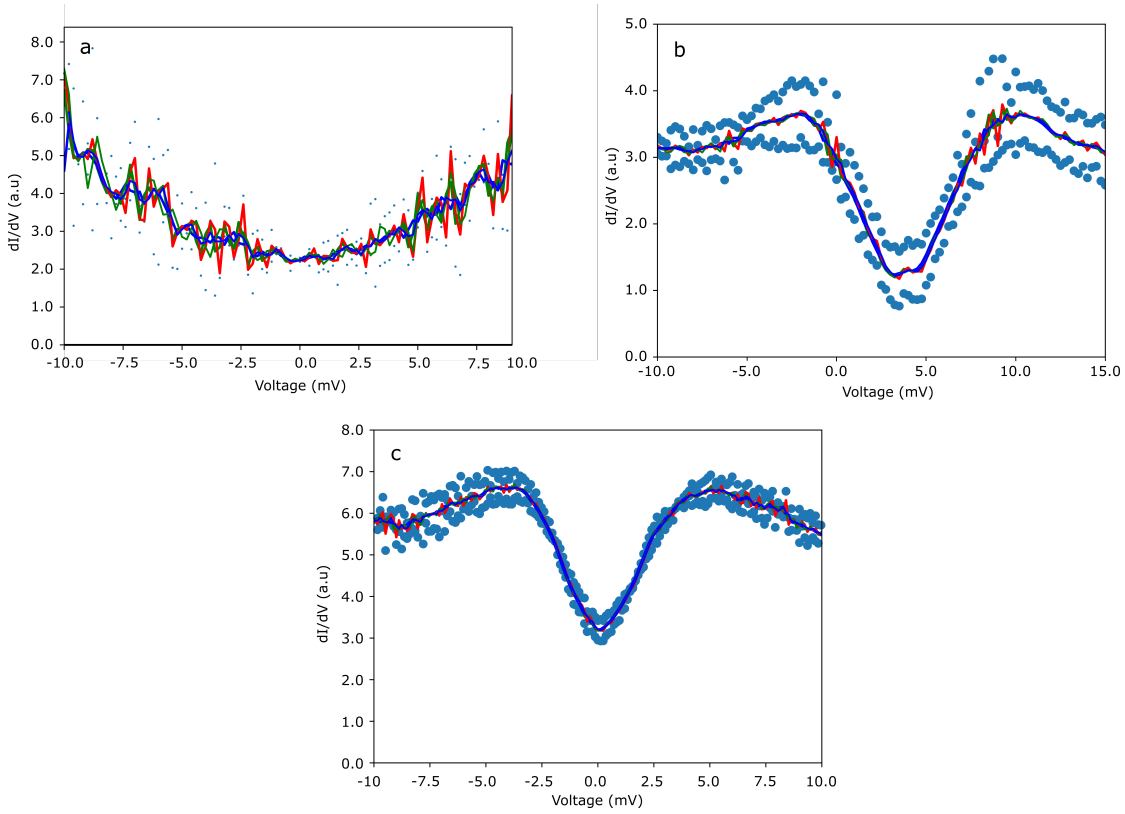

Figure 12: (a,b,c) dI/dV spectrum taken on Pb(100) at the voltage range at which a superconducting gap is expected. (a) Due to high frequency noise the SC gap is not visible. (b) After reducing the high frequency noise, a superconducting gap of $6mV$ is visible, however not at the 0V point. (c) Same spectrum as (b),except the correct location of the SC gap is shown. This spectrum was taken by Albrecht Feltz.

5 Summary and Conclusion

In this report it was shown what is needed to create a working STM machine and which possible problems one might encounter while operating this machine. In order to make the POLAR STM fully operational we reduced the noise level to 2pm peak to peak. We identified the frequencies of the noise on the built-in oscilloscope and one by one found solutions to reduce the noise. We used filters, noise dampening feet and ferrite core cables to reduce the noise level. After the noise was reduced, we showed that it is possible to clean both Cu(111) and Pb(100) with annealing and sputtering with argon ions and that atomic resolution images can be taken of the clean crystals. We also showed that it is possible to do Scanning Tunneling Spectroscopy on Cu(111) and Pb(100). We showed it was possible to visualize the surface state of Cu(111) and the superconducting gap of Pb(100). From these spectra is was concluded that the high frequency noise was reduced and did not interfere with the measurement. CO molecules were evaporated on a Cu(111) crystal and we showed manipulation of these molecules. Lastly we showed that atomic manipulation was also possible with Pb adatoms on the Pb(100) surface and that CO molecules do not adsorb to the lead crystal surface. From this result we concluded that Pb(100) is an unsuitable crystal for creating artificial lattices of CO on the surface.

6 Outlook

Due to currently running, unpublished, research this part of the thesis has been removed.

7 Acknowledgments

First of all I want to thank Ingmar Swart and Daniël Vanmaekelbergh for the opportunity to work on the STM and for all the advice during the research. Of course I also want to thank my daily supervisor Thomas who taught me how to work on the STM and made sure both me and the machine did not suffer any damage. A big thanks to Saoirsé, Marlou, Peter, Pascal, Pierre, Jan-Jurre and the other members of Team Kelder for all the discussions, help and moments of laughter. A special thanks to Pascal for running the simulation of CO on lead. Thanks also to Peter v/d Beld for installing all kinds of different Swagelok components on the STM.

References

[1] P.H. Hofmann. The surfaces of bismuth: Structural and electronic properties. *Progress in Surface Science*, 81(5):191–245, 2006.

[2] M. Kopciuszyński, R. Zdyb, P. Nita, M. Dachniewicz, and P. Dyniec. Quasi one-dimensional lead ribbons on the Si(110) surface. *Applied Surface Science*, 373:8–12, 2016.

[3] P.H. Jacobse, M.J.J Mangnus, S.J.M Zevenhuizen, and I. Swart. Mapping the Conductance of Electronically Decoupled Graphene Nanoribbons. *ACS Nano*, 12(7):7048–7056, 2018.

[4] Y. Fei, K.L. Bu, W.H. Zhang, Y. Zheng, X. Sun, Y. Ding, X.J. Zhou, and Y. Yin. Electronic effect of doped oxygen atoms in Bi2201 superconductors determined by scanning tunneling microscopy. *Science China: Physics, Mechanics and Astronomy*, 61(12), 2018.

[5] G. Binning, H. Rohrer, Ch. Gerber and E. Weibel. Surface Studies by Scanning Tunneling Microscopy. *Search of Excellence*, 49(1):57–61, 1982.

[6] S. D. Kevan and R. H. Gaylord. High-resolution photoemission study of the electronic structure of the noble-metal (111) surfaces. *Physical Review B*, 36(11):5809–5818, 1987.

[7] K. Morgenstern, N. Lorente, and K.H. Rieder. Controlled manipulation of single atoms and small molecules using the scanning tunnelling microscope. *Physica Status Solidi (B)*, 250(9):1671–1751, 2013.

[8] G. Hörmandinger. Imaging of the Cu(111) surface state in scanning tunneling microscopy. *Physical Review B*, 49(19):13897–13905, 1994.

[9] K.K. Gomes, W. Mar, W. Ko, F. Guinea, and H.C. Manoharan. Designer Dirac fermions and topological phases in molecular graphene. *Nature*, 2012.

[10] M.R. Slot, T.S. Gardenier, P.H. Jacobse, G.C.P. Van Miert, S.N. Kempkes, S.J.M. Zevenhuizen, C.M. Smith, D.A.M Vanmaekelbergh, and I Swart. Experimental realization and characterization of an electronic Lieb lattice. *Nature Physics*, 2017.

[11] G. W. Webb, F. Marsiglio, and J. E. Hirsch. Superconductivity in the elements, alloys and simple compounds. *Physica C: Superconductivity and its Applications*, 514:17–27, 2015.

[12] E.j. Heller, D. Eigler, M.f. Crommie, and C.p. Lutz. Scattering and absorption of surface electron waves in quantum corals. *Nature*, 368:561 – 563, 1994.

[13] J Van der Lit. *Non-contact AFM and STM studies of molecular systems on weakly interacting surfaces : Can't touch this!* PhD thesis, Utrecht University, 2016.

[14] S.W. Hla. Atom-by-atom assembly. *Reports on Progress in Physics*, 77(5), 2014.

[15] C. B. Samantaray. Scanning probe microscopy for nanolithography. *Surface Science Tools for Nanomaterials Characterization*, pages 91–115, 2015.

[16] C. Krull. *Electronic Structure of Metal Phthalocyanines on Ag(100).* PhD thesis, 2014.

[17] P. Wahl, L. Diekhöner, M. A. Schneider, and K. Kern. Background removal in scanning tunneling spectroscopy of single atoms and molecules on metal surfaces. *Review of Scientific Instruments*, 79(4), 2008.

[18] M. Ruby, B.W. Heinrich, J. I. Pascual, and K.J. Franke. Experimental demonstration of a two-band superconducting state for lead using scanning tunneling spectroscopy. *Physical Review Letters*, 2015.

[19] S. DeVore, A. Gauthier, J. Levy, and C. Singh. Improving Students' Understanding of Lock-In Amplifiers. *2013 Physics Education Research Conference Proceedings*, 15260:121–124, 2014.

[20] D.M. Eigler and E.K. Schweizer. Positioning single atoms with a scanning tunneling microscope, 1990.

[21] C. P. Lutz M. F. Crommie and D. M. Eigler. Confinement of Electrons to Quantum Corrals on a Metal Surface. 220(4598):671–680, 1993.

[22] G. Meyer, L. Bartels, and K.H. Rieder. Atom manipulation with the STM: Nanostructuring, tip functionalization, and femtochemistry. *Computational Materials Science*, 20(3-4):443–450, 2001.

[23] R.J. Celotta, S. B. Balakirsky, A.P. Fein, F.M. Hess, G.M. Rutter, and J.A. Stroscio. Invited Article: Autonomous assembly of atomically perfect nanostructures using a scanning tunneling microscope. *Citation: Review of Scientific Instruments*, 85, 2014.

[24] G. Meyer, L. Bartels, S. Zoephel, and R. Karl-Heinz. Possibilities for atom by atom restructuring of surfaces employing native substrate atoms as well as foreign species. *Applied Surface Science*, 1998.

[25] T.S. Gardenier. *The electronic structure of an artificial electronic Lieb lattice*. Master thesis, Utrecht University, 2016.

[26] M. Bos. *A search for an atomically flat Pb surface*. Bachelor thesis, Utrecht University, 2017.

[27] S. Tewari, K.M. Bastiaans, M. P. Allan, and J.M. van Ruitenbeek. Robust procedure for creating and characterizing the atomic structure of scanning tunneling microscope tips. *Beilstein Journal of Nanotechnology*, 8(1):2389–2395, 2017.

[28] F. Bustamante and C. Biscarini. Scanning tunneling microscopy. II. Calculation of images of atomic and molecular adsorbates. *Physical Review B*, 51(16), 1995.

[29] B. Wortmann, D. van Vorden, P. Graf, R. Robles, P. Abufager, N. Bobisch, Lorente C. A., and R Möller. Reversible 2D Phase Transition Driven By an Electric Field: Visualization and Control on the Atomic Scale. *Nano Letters*, 16(16):528–533, 2016.

[30] L Bartels, G Meyer, and K.-H. Rieder. Controlled vertical manipulation of single CO molecules with the scanning tunneling microscope: A route to chemical contrast. *Applied Physics Letters*, 71(2):213–215, 1997.

[31] K. Wurde, A. Mazur, and J. Pollmann. Surface electronic states of Pb(001), Pb(110),. *Physical Review B*, 49(11):7679–7686, 1994.

[32] Cooper. L. Bound electron pairs in a degenerated fermi gas. *Physical Review*, 104(4):1189–1190, 1956.

[33] J. Bardeen, L.N. Cooper, and J.R. Schrieffer. The microscopic theory of superconductivity. *Contemporary Physics*, 9(6):549–564, 1968.

[34] Ji. Liu, X. Wu, F. Ming, X. Zhang, K. Wang, B. Wang, and X. Xiao. Size-dependent superconducting state of individual nanosized Pb islands grown on Si(111) by tunneling spectroscopy. *Journal of Physics Condensed Matter*, 23(26), 2011.